

# Orbit-Determination Performance of Doppler Data for Interplanetary Cruise Trajectories

## Part II: 8.4-GHz Performance and Data-Weighting Strategies

J. S. Ulvestad  
Navigation Systems Section

*A consider error covariance analysis has been performed in order to investigate the orbit-determination performance attainable using two-way (coherent) 8.4-GHz (X-band) Doppler data for two segments of the planned Mars Observer trajectory. The analysis includes the effects of the current level of calibration errors in tropospheric delay, ionospheric delay, and station locations, with particular emphasis placed on assessing the performance of several candidate elevation-dependent data-weighting functions. One weighting function has been found that yields good performance for a variety of tracking geometries. This weighting function is simple and robust; it reduces the danger of error that might exist if an analyst had to select one of several different weighting functions that are highly sensitive to the exact choice of parameters and to the tracking geometry. Orbit-determination accuracy improvements that may be obtained through the use of calibration data derived from Global Positioning System (GPS) satellites also have been investigated, and can be as much as a factor of three in some components of the spacecraft state vector. Assuming that both station-location errors and troposphere calibration errors are reduced simultaneously, the recommended data-weighting function need not be changed when GPS calibrations are incorporated in the orbit-determination process.*

### I. Introduction

Two-way Doppler data are the primary data type used for the navigation of robotic spacecraft during the interplanetary cruise portions of their trajectories. Empirically, it has been found that data acquired at very low elevation angles at a given tracking station can degrade the accu-

racy of the determination of a spacecraft trajectory. In the case of data taken at 2.3 GHz (S-band), the degradation occurs primarily because of errors in the calibration of the Earth's ionosphere and the interplanetary charged-particle medium, while for 8.4-GHz (X-band) data, errors in the troposphere calibration generally cause the largest Doppler measurement errors at low elevations. Therefore,

traditional practice has been to (1) impose an arbitrary elevation-angle cutoff, below which all data are discarded; or (2) apply a data-weighting function that reduces the weighting of the low-elevation data by increasing the variances assigned to Doppler measurements made at decreasing elevation angles.

Reference [1] described a consider covariance analysis methodology that was developed to investigate the effects of different Doppler weighting functions on orbit-determination accuracy for interplanetary cruise trajectories. This article reports results obtained by applying that covariance analysis to two different portions of a hypothetical trajectory for the Mars Observer mission [2], which is scheduled to be launched toward Mars in September 1992 and to arrive in September 1993. It is assumed that two-way Doppler data will be acquired at 8.4 GHz by the DSN. The calibration errors are those expected in such data during normal DSN operations in 1992 and 1993. Tracking sessions (“passes”) are assumed to take place at a single Deep Space Station (either Goldstone, California, or Tidbinbilla, Australia) on 10 consecutive days. In each case, the error covariance matrix is calculated for the determination of the spacecraft state vector at an epoch defined to be the midpoint of the first of the 10 passes.

Section II of this article gives a brief review of the covariance analysis procedure developed in [1], including a definition of the data-weighting function. Section III summarizes the justification for the assumptions about the current level of calibration errors. In Section IV, a general description is given of the data arcs and assumptions employed for calculation of the error covariance matrices. Section V describes the results of the analysis for a near-zero-declination segment of the Mars Observer trajectory, while Section VI presents similar results for a high-declination trajectory segment. Section VII gives the results of an investigation of the benefits that might be obtained by reducing various calibration errors through the use of Global Positioning System (GPS) satellites or water-vapor radiometers. Section VIII provides some discussion of the results and provides a recommended weighting function for 8.4-GHz Doppler data for Mars Observer and other interplanetary spacecraft. Section IX summarizes the results and indicates some possible directions for future work.

## II. Covariance Analysis and the Weighting Function

### A. Introductory Remarks

The consider covariance error analysis used to investigate the sample trajectories was described in [1], and the

reader is referred to that article for details. (Also, see [3].) For each data arc, four parameters were extracted from the final covariance matrix in order to characterize the quality of the estimated spacecraft trajectory. Those four were the uncertainty in the line-of-sight position and velocity of the spacecraft as well as the lengths of the major axes of the position and velocity error ellipses in the plane of the sky, that plane perpendicular to the Earth-spacecraft line of sight. These errors are expressed in a Cartesian plane-of-sky frame rather than a spherical-coordinate frame. Thus the error in the line-of-sight velocity appears greater than it would in a spherical coordinate system because of the uncertainty in the direction of the line-of-sight coordinate axis.

### B. Weighting Function

The weighting function used for a particular Doppler point has been given the form

$$w = \left[ \sigma_D^2 + \left( \frac{\sigma_e}{(\sin \gamma)^q} \right)^2 \right]^{-1} \quad (1)$$

for elevation angles  $\gamma$  above a user-selected cutoff  $\gamma_{\min}$ , and zero at lower elevations (i.e., the data at elevations below  $\gamma_{\min}$  were discarded). In Eq. (1),  $\sigma_D$  is the assumed Doppler data noise (including any possible deweighting that is independent of elevation),  $\gamma$  is the elevation angle of the spacecraft,  $\sigma_e$  is a constant that determines the importance of the elevation-dependent part of the weighting function, and  $q$  is a parameter governing the form, or “steepness,” of that dependence. The user has the ability to vary four different parameters ( $\sigma_D$ ,  $\sigma_e$ ,  $\gamma_{\min}$ , and  $q$ ) in order to optimize results. Of course,  $\sigma_D$  must be no smaller than the precision of the Doppler measurements, while  $\gamma_{\min}$  must be no smaller than the lowest elevation at which the DSN antennas can operate.

The chosen form of the weighting function is based on the behavior of the static troposphere calibration error as it varies with elevation, and to a lesser extent, the behavior of ionosphere calibration errors as well. The weighting function for various choices of parameters in Eq. (1) was plotted in [1], as was the shape of the partial derivatives of the Doppler measurements with respect to errors in the media calibration. In [1], it was shown that troposphere calibration error was the dominant media effect at 8.4 GHz for low-elevation angles.

### III. Assumed Error Magnitudes

The level of random measurement noise in the Doppler data and the magnitude of the calibration errors must be

assumed in order to estimate the errors in the spacecraft state vector at the reference time. The one-sigma noise on the Doppler data was taken to be 0.1 mm/sec over an assumed integration time of 60 seconds, typical of the data noise seen in 8.4-GHz, two-way Doppler data acquired from the Magellan spacecraft.<sup>1</sup>

The one-sigma errors in the calibration of the zenith path delay due to the wet and dry troposphere were taken to be 4 cm and 1 cm, respectively. These errors are typical of those obtained from current calibration methods using measurements of atmospheric pressure, temperature, and relative humidity. There is some potential for reducing the error in the wet component, which tends to be the dominant error source, through the use of water-vapor radiometers [4] or GPS satellites [5].

The partial derivatives of Doppler measurements with respect to ionosphere calibration errors can be written in terms of two coefficients that represent (approximately) the uncertainties in the daytime and nighttime delays at the zenith. The calibration errors were taken to be 4 cm for the daytime coefficient and 2 cm for the nighttime coefficient, the approximate levels achievable using the current Faraday rotation measurements at the DSN Deep Space Stations [6]. At 2.3 GHz, the uncertainty in these coefficients would be a factor of  $\sim 13$  higher because of the dependence on the square of the wavelength. GPS observations could improve these calibrations in the future [7].

The final calibration error considered is the location of the tracking station. This error source also can represent to some degree the error in the calibration of Universal Time and Polar Motion, since the partial derivatives are similar. An error in timing is equivalent to an error in the station longitude, while an error in the position of the Earth's pole will effectively manifest itself as an error in the tracking-station position relative to the pole. In the calculations presented below, the errors in the equatorial components of the station locations were assumed to be 30 cm, while the error in the z-component (toward the pole) relative to the Earth's center was taken to be 5 m. The assumed errors in the equatorial plane are slightly conservative for station locations alone, but are reasonable values when current Earth-orientation errors also are included. As with the other calibration errors, GPS observations conceivably could provide substantial reductions in uncertainty [8,9]. All the calibration errors given here

are assumed in Sections V and VI; they are summarized in Table 1.

## IV. Data Arcs

All the analyses described in this article are based on one of two segments of a hypothetical Mars Observer trajectory. One segment begins at a declination near 20 deg, while the other starts near 5 deg declination. These two cases were studied because the well-known lack of sensitivity of Doppler data to the spacecraft declination for trajectory segments near the celestial equator (e.g., [10]) could lead to different conclusions for the high- and near-zero-declination cases.

For each trajectory segment, the error covariance matrices were calculated for data arcs consisting of 10 consecutive days of two-way (coherent) 8.4-GHz Doppler data acquired using a single tracking station. The reference epoch for each data arc was taken to be the midpoint of the tracking pass on the first day of that arc. For each data arc, cases were computed for low-elevation cutoffs ranging from 6 deg to 40 deg; all ten passes within a data arc were assumed to have the same cutoff. Contiguous 60-second Doppler data points were assumed to be acquired for the entire length of each pass; the magnitude of the data noise and the assumed calibration errors were as described in Section III. Combination of data from more than one tracking station goes beyond the scope of this work and was not considered. However, the cases of tracking from a Northern Hemisphere site (Goldstone, California, at a latitude of approximately +35 deg) and from a Southern Hemisphere site (Tidbinbilla, Australia, at a latitude of approximately -35 deg) were both considered. The coordinates assumed for the tracking stations are given in Table 2.<sup>2</sup>

## V. Near-Zero-Declination Mars Observer Trajectory Segment

The near-zero-declination segment of the Mars Observer trajectory begins on Day 203 (22 July) of 1993. The initial geocentric state vector, in spherical coordinates, is given in Table 3. The initial spacecraft declination is 5.1 deg, but the initial declination rate of approximately -0.22 deg/day implies that the spacecraft declination is near 3.1 deg by the end of the 10-day data arc.

<sup>1</sup> G. R. Kronschnabl, "Magellan Differenced Doppler Data Quality Evaluation," Interoffice Memorandum 3140-GRK-90-011 (internal document), Jet Propulsion Laboratory, Pasadena, California, May 24, 1990.

<sup>2</sup> T. D. Moyer, "Station Location Sets Referred to the Radio Frame," Interoffice Memorandum 314.5-1334 (internal document), Jet Propulsion Laboratory, Pasadena, California, February 24, 1989.

## A. Tracking From Goldstone

First, consider the case in which Doppler data are acquired only from Goldstone. Although the bulk of the results in this article will be given only in figures, inspection of the results in a tabular form also can be instructive. Therefore, the computed uncertainties for the line-of-sight spacecraft position for a variety of weighting functions are compiled in Table 4. Eleven different cases are included in this table, each having the same initial spacecraft state vector. Eight different elevation-angle cutoffs were considered for each case. The first row of numbers gives the results for a covariance analysis including only the data-noise component of the measurement errors and having uniform data weighting. The remaining ten cases all include the calibration and random measurement error levels listed in Table 1.

As expected, the result for the case in which only data noise is included improves as the elevation cutoff is reduced; i.e., taking more data of uniform quality always helps, hardly a surprising result. However, if the same uniform weighting is applied to data in the presence of unmodelled media calibration errors, the large systematic Doppler measurement errors at low elevations make the result substantially worse when all the data are included (cf. second row of Table 4). The data analyst's first and most obvious recourse would be to discard the low-elevation data. An alternative of uniformly deweighting all of the Doppler data flattens the shape of the dependence on elevation cutoff, but only at the expense of making the results *worse* for all values of the cutoff. The third row of Table 4 shows the results for uniform deweighting from 0.1 mm/sec to 0.2 mm/sec. In fact, the data would have to be uniformly deweighted to approximately 0.5 mm/sec to remove the bulk of the dependence on the selected elevation cutoff.

Of course, the point of this investigation is to explore the benefits of nonuniform data deweighting. Results for eight choices of parameters in the weighting function (Eq. [1]) are given in the last eight rows of Table 4. As might be expected, when the data weighting is not strongly dependent on elevation angle ( $q = 1$ ), the low-elevation data still corrupt the line-of-sight position estimates significantly. Although the results for a high-elevation cutoff can be as good as those for the steeper weighting functions, achievement of the best results still depends greatly on the exact choice of the elevation cutoff. This lack of robustness leads to a strong preference for lower weighting of the low-elevation data. In fact, for a weighting function having  $q = 3$ , the expected errors are almost independent of the elevation cutoff and also change little when the coefficient  $\sigma_e$  is varied by a factor of five between 0.01 mm/sec

and 0.05 mm/sec. The lack of dependence on the selection of the elevation cutoff occurs because the steep weighting function already has the effect of almost completely discarding the data at the lower elevations, making the specification of the cutoff superfluous.

Figures 1(a-d) display results for the four figures of merit generally used in this analysis, radial position and velocity errors, and the semimajor axes of the position and velocity error ellipses in the plane of the sky. In each figure, six curves are plotted. Curve A is the predicted result for perfect calibration of the troposphere, ionosphere, and station location. Curve B assumes standard calibration errors and uniform data weighting for a noise level of  $\sigma_D = 0.1$  mm/sec. Curves C, D, and E all are based on standard calibration errors and  $\sigma_e = 0.03$  mm/sec. Curve C has  $q = 1$  in Eq. (1), curve D has  $q = 2$ , and curve E has  $q = 3$ . Finally, curve F corresponds to uniform weighting with the Doppler data deweighted to  $\sigma_D = 0.2$  mm/sec.

In Fig. 1, the shapes of the curves as functions of weighting function and elevation cutoff angle look similar for both line-of-sight coordinates and for the plane-of-sky position. One can find differences in detail, but the general conclusions are similar for all three quantities. As expected for the near-zero-declination case, the error in the plane-of-sky position is predominantly in the declination direction, with its major axis within 15 deg of the declination axis in all cases.

The result for the plane-of-sky velocity error [Fig. 1(d)] has a different character. Even in the absence of calibration errors, this quantity is relatively poorly determined by the Doppler measurements over a short data arc, often a factor of more than 30 worse than the line-of-sight velocity. This occurs because the spacecraft plane-of-sky motion must be inferred indirectly from the spacecraft's Doppler signature over the course of the data arc, while the epoch line-of-sight velocity is measured much more directly, since the Doppler shift effectively is equivalent to the station-spacecraft range rate. The media and station-location calibration errors have little impact on the overall accuracy of determination of the plane-of-sky velocity, and deweighting or discarding low-elevation data causes a loss of information that would help provide a more accurate result. The best result for the plane-of-sky velocity is achieved in this case by choosing  $q = 1$  and using data acquired at the lowest possible elevation angles.

## B. Tracking From Australia

The results for tracking data from the Tidbinbilla, Australia, DSN site are quite similar to the results for tracking

data from Goldstone. In general, the expected errors are 5 to 10 percent higher for the Australia data, with dependences on the weighting functions that are virtually identical to those in the Goldstone case. Because of the similarity to the results for Goldstone, no plots are shown for the case of tracking from Australia. The slight decrease in accuracy is due to the shorter tracking passes from the southern DSN site for a spacecraft that is a few degrees north of the equator; the difference in tracking pass length ranges from 1 to 1.5 hours, depending on the elevation cutoff selected.

## VI. High-Declination Mars Observer Trajectory Segment

The high-declination segment of the Mars Observer trajectory begins on Day 113 (23 April) of 1993, with an initial spacecraft declination of about 20.3 deg. Initial conditions for the spacecraft state are given in Table 5. Over the course of the 10-day data arc, the spacecraft declination decreases to about 19.5 deg.

### A. Tracking From Goldstone

Figures 2(a–d) display the results for the 4 standard figures of merit in the case of 10 consecutive tracking passes from Goldstone. Predicted orbit-determination accuracy is a factor of 2 to 8 better than that for the near-zero-declination trajectory segment, depending on the specific component and the weighting function being investigated. (Note that the spacecraft distance from Earth is only 60 percent of its distance during the near-zero-declination trajectory segment.) A notable difference [Fig. 2(a)] is that the line-of-sight position error is quite close to the results for data noise only, implying that the current calibration errors have relatively little effect on the determination of this quantity using two-way Doppler data. For this case, the weighting functions with little deweighting at low elevations (i.e.,  $q = 1$  rather than 2 or 3) give the best results, since the power of the extra data is more important than the small increase in errors due to miscalibration. However, results for  $q = 2$  are close to the results for  $q = 1$  for both line-of-sight position and plane-of-sky velocity [Figs. 2(a) and 2(d)], while they are somewhat better for the other two variables [Figs. 2(b) and 2(c)]. In general, the specific choice of weighting functions is much less important than it is for the near-zero-declination case. Some deweighting of the low-elevation data still is important, however, in order to prevent sharp upturns in the trajectory uncertainty plots when data below 10 deg elevation are included in the orbit solutions.

### B. Tracking From Australia

One might expect the tracking from Australia to give somewhat poorer results than that from Goldstone because of the abbreviated tracking passes (8.8 hours instead of 12.9 hours for tracking down to 6 deg elevation) and because of the larger amount of low-elevation data. While this is generally true, the degradation in performance is not very great. In fact, the Australia data give performance a factor only 1.2 to 2 poorer than the Goldstone data for all figures of merit. When the line-of-sight position error is considered for the cases in which there is little deweighting, the performance degradation factor of  $\sim 1.2$  is roughly the square root of the difference in tracking-pass lengths, as expected for the situation in which the results are dominated by data noise.

Figures 3(a–d) show results for several different weighting functions. The best results for both line-of-sight position and plane-of-sky velocity [Figs. 3(a) and 3(d)] for the Australia track are achieved by applying no data deweighting and using data acquired at elevation angles as low as 6 deg. Some deweighting is useful for the line-of-sight velocity [Fig. 3(b)], and it is especially important for the plane-of-sky position [Fig. 3(c)]. Results for  $q = 2$  appear to be best and are 20 to 40 percent better than those for the case with  $q = 1$ ; the cases having  $q = 2$  are about 20 to 40 percent *worse* than those for  $q = 1$  when the line-of-sight position and plane-of-sky velocity are considered. Deweighting the low-elevation data too much actually degrades the accuracy of the latter two components of the state vector because they depend more on data noise than on the accuracy of the calibration of systematic errors.

## VII. Effects of Improved Calibration

It is well-known that measurements derived from the GPS satellites have the potential for improving the calibration of some of the effects that lead to errors in Doppler data [5,7–9]; water-vapor radiometers [4] also might offer some improvement in the calibration of the wet troposphere. The orbit-determination improvement that might be obtained has been investigated by reducing the levels of the troposphere calibration errors and the station-location errors, both individually and together, in the analyses described in Sections V and VI. Reductions in ionosphere calibration errors have not been considered because they have less effect on 8.4-GHz data. The calibration improvements that were considered were a decrease from 4 cm to 1 cm in the calibration error for the zenith delay due to the wet troposphere, and an improvement to 5 cm in the knowledge of each of the three station-location components.

Doppler tracking from Goldstone with improved calibration of the systematic errors has been investigated for both the near-zero- and high-declination cases. (Results for tracking from Australia would be similar.) For the near-zero-declination trajectory segment, Figs. 4(a-d) show a sample of results for cases in which the wet-troposphere and station-location calibrations were improved by the amounts specified above. Curve A is the comparison curve for uniform weighting with  $\sigma_D = 0.1$  mm/sec, derived under the assumption of perfect calibration. Curve B shows the results for a weighting function having  $\sigma_e = 0.03$  mm/sec,  $q = 2$ , and  $\sigma_D = 0.1$  mm/sec, assuming the current calibration errors given in Table 1. Curve C shows the results for the same weighting function with the zenith wet troposphere calibration error reduced from 4 cm to 1 cm, curve D shows results with the station-location calibration errors reduced to 5 cm per component, and curve E shows the results when both the station-location and troposphere calibrations are improved simultaneously.

It is apparent that improving the station-location calibration to 5 cm per component provides a greater error reduction than does the improvement from 4 cm to 1 cm in the calibration of the wet troposphere. A more detailed investigation would be necessary to assess the value of incremental improvements, say, improving the wet troposphere calibration from 4 cm to 3 cm or the  $z$ -component of the station-location error from 5 m to 50 cm. Improving both calibrations to levels that may be achievable using observations of GPS satellites can reduce the orbit-determination errors by as much as a factor of three for some parameters.

Figures 4(a-c) show that when only the station location calibrations are improved, a weighting function having  $q = 2$  actually does not completely flatten the dependence on the elevation-angle cutoff. This clearly is because the troposphere calibration error dominates the orbit-determination error for this case, and the low-elevation data should have even lower weights. Although the weighting function with  $q = 3$  (not shown) actually would be a better choice when only the station-location errors are reduced,  $q = 2$  is the preferred choice when both station-location and troposphere calibration errors are reduced.

Investigation of the high-declination trajectory segment shows similar improvements from reducing the calibration errors, as displayed in Figs. 5(a-d). Again, the improvement in the station-location calibration yields the biggest gain. Naturally, the improvements are less in the parameters already dominated by data noise rather than by calibration errors. But improvement by more than a factor of three still is possible for the plane-of-sky position.

## VIII. Discussion

The figures and tables presented in the preceding sections showed results for a variety of assumptions. However, for the current level of calibration errors, the general character of the results did not change significantly over the different cases considered. In particular, inspection of Figs. 1-3 shows that the curves labelled D generally have the best combination of attributes for the line-of-sight and plane-of-sky position and velocity uncertainties. For low-elevation cutoffs, these curves show a significant reduction of errors over the uniformly weighted case. They also appear quite flat as a function of the selected elevation cutoff. Therefore, the weighting function labelled D appears to be a good choice for 8.4-GHz Doppler data with noise of 0.1 mm/sec that is affected by calibration errors at the levels assumed herein. The parameters of this weighting function are  $\sigma_D = 0.1$  mm/sec,  $\sigma_e = 0.03$  mm/sec, and  $q = 2$ .

For the near-zero-declination trajectory and tracking from Goldstone, Figs. 6(a) and 6(b) show the respective dependence of predicted position and velocity accuracies on  $\sigma_e$ , assuming a low-elevation cutoff of 6 deg,  $q = 2$ , and  $\sigma_D = 0.1$  mm/sec. Note that the predicted errors in both position components and in the line-of-sight velocity actually are smallest for  $\sigma_e = 0.05$  mm/sec, but vary by less than  $\sim 10$  percent for  $\sigma_e$  between 0.02 and 0.05 mm/sec. The plane-of-sky velocity, on the other hand, is dominated by the data noise and is determined most accurately for  $\sigma_e = 0.01$  mm/sec. The choice of  $\sigma_e = 0.03$  mm/sec appears to be a good compromise. If the plane-of-sky velocity is not a parameter of great interest,  $\sigma_e = 0.05$  mm/sec would be a slightly better choice. The trajectory solution statistics seem fairly robust for choices of  $\sigma_e$  between 0.02 and 0.05 mm/sec; the best selection for real orbit-determination analysis should be established by making tests with actual spacecraft data rather than relying solely on a covariance analysis.

Based on the results of the analysis, the following weighting function is recommended for 8.4-GHz two-way Doppler data acquired from Mars Observer:

$$w = \left[ (0.1 \text{ mm/sec})^2 + \left( \frac{0.03 \text{ mm/sec}}{\sin^2 \gamma} \right)^2 \right]^{-1} \quad (2)$$

where  $\gamma$  is the elevation angle. All data down to the lowest possible elevation angle should be included in orbit-determination calculations. The above weighting function also is recommended for the interplanetary cruise trajectory of any other mission having calibration errors

similar to those expected for Mars Observer. The recommendation holds for trajectories at different declinations and for tracking from any of the three main DSN complexes (California, Australia, or Spain). Operational orbit-determination software should incorporate a weighting function of the above form, with some capability for analysts to vary the parameters slightly as necessary to achieve the best estimated trajectory.

Analysts processing the actual data for missions such as Mars Observer might find slight improvements in the results by varying the parameters in Eq. (2). For instance, they may find that the data below 10-deg elevation angles seem to corrupt their solutions, possibly because the effects of the troposphere calibration errors have been underestimated or because the time-varying component of the troposphere (not considered in the work presented here) affects the data. A somewhat larger value of  $\sigma_e$  or a cutoff in elevation angle may improve the results under those circumstances. Of course, given that other data types such as ranging and Very Long Baseline Interferometry (VLBI) sometimes are included in the orbit-determination process, the best weighting function for 8.4-GHz Doppler data when multiple data types are used could be slightly different from that shown in Eq. (2).

Perhaps the most significant attribute of the weighting function recommended here is that it removes almost all dependence on the selection of an elevation-angle cutoff. In fact, the magnitudes of the predicted errors are quite similar to the errors expected for uniformly weighted data *if* the proper elevation cutoff is selected. However, the recommended solution is more robust, virtually removing the possibility of corrupting the estimated trajectory due to a poor choice of the elevation cutoff. In fact, in the case of uniformly weighted data, a much lower elevation-angle cutoff generally would be preferred for determining the plane-of-sky velocity than for the other orbit parameters, making it quite difficult to choose the best compromise. In addition, dependence of the preferred weighting function on the identity of the station is eliminated when Eq. (2) is used as the weighting function. If uniform weighting were used for a high-declination trajectory, the preferred elevation cutoff for tracking from Australia would be considerably lower than that for tracking from California, and there would be a risk that the wrong choice of cutoff angles might be made for the different stations.

Elimination of the elevation-angle cutoff also is beneficial from a navigation standpoint because the inclusion of all possible data yields longer effective passes from each station. Although only the interplanetary cruise phase has been analyzed, it is likely that a weighting function simi-

lar to Eq. (2) would be helpful in planetary approach and encounter scenarios, when trajectory solutions sometimes must be generated from only a few passes of data. Longer passes would provide more sensitivity to spacecraft acceleration caused by a planet's gravitational field.

For the cases in which improved calibrations are assumed, the weighting function shown in Eq. (2) also seems to give good results. Greater deweighting of the elevation data ( $q = 3$ ) might be preferable for the case in which only the station-location calibration is improved. However, if it is assumed that the troposphere and station-location calibration errors are reduced at approximately the same time (for instance, both by using GPS-based calibration data), a weighting function similar to that specified in Eq. (2) still seems to be a good choice.

## IX. Summary and Directions for Future Work

This article has reported the results of a covariance analysis of the use of 8.4-GHz Doppler data for orbit determination in the interplanetary cruise phase of a mission. Investigation of a variety of data-weighting functions has resulted in selection of an elevation-dependent data-weighting scheme. Predicted accuracies are similar to those that conceivably could be achieved with uniformly weighted data and a cutoff at high-elevation angles. However, use of the recommended weighting function and inclusion of data taken at all elevations enhances the robustness of the orbit-determination process. The same weighting function will work well for high- and near-zero-declination data and for all DSN tracking stations. Thus the recommended weighting function greatly reduces the sensitivity of the estimated trajectory to choices left to the data analyst's discretion.

The results presented here represent a simplified case that still should be applicable to the more complex circumstances encountered in operational orbit determination. However, specific analyses should be performed for more complicated situations. The list below suggests several areas in which future work would be beneficial.

- (1) Analyze the results obtainable for a 10-day data arc including Doppler data taken from all three DSN sites, not just one of those sites.
- (2) Analyze the accuracy obtainable at 32 GHz, with lower data noise and a variety of assumptions about the calibration errors.
- (3) Extend the analysis method to include the gravitational influence of another planet, enabling applica-

tion of the calculations to the planetary approach case.

- (4) Perform a similar analysis for other data types, such as range and VLBI.
- (5) Combine the different data types to find an optimal weighting for each in the presence of the other data in the orbit-determination solutions.

The analysis suggested in items (1) and (2) above represents a fairly straightforward extension of this article and [1]. However, items (3–5) all require significant increases in model and computational complexity. Thus, they would make it more difficult to consider a large number of different cases in a short period. The desirability of spending the effort necessary to make those investigations has not yet been established.

## Acknowledgments

The author thanks Stuart Demczak for supplying the Mars Observer trajectory used for the studies in this article, and Sam Thurman for many helpful discussions and critical readings of earlier drafts of the article.

## References

- [1] J. S. Ulvestad and S. W. Thurman, "Orbit-Determination Performance of Doppler Data for Interplanetary Cruise Trajectories, Part I: Error Analysis Methodology," *TDA Progress Report 42-108*, vol. October–December 1991, Jet Propulsion Laboratory, Pasadena, California, pp. 31–48, February 15, 1992.
- [2] M. Meham, "Mars Observer Begins New Era Using Proven Spacecraft Design," *Aviation Week and Space Technology*, vol. 131, no. 15, pp. 79–82, October 9, 1989.
- [3] V. J. Ondrasik and D. W. Curkendall, "A First-Order Theory for Use in Investigating the Information Content Contained in a Few Days of Radio Tracking Data," *Deep Space Network Progress Report*, JPL Technical Report 32-1526, vol. III, pp. 77–93, June 15, 1971.
- [4] J. M. Moran and B. R. Rosen, "Estimation of the Propagation Delay Through the Troposphere from Microwave Radiometer Data," *Radio Science*, vol. 16, no. 2, pp. 235–244, March–April, 1981.
- [5] S. M. Lichten, "Precise Estimation of Tropospheric Path Delays With GPS Techniques," *TDA Progress Report 42-100*, vol. October–December 1989, Jet Propulsion Laboratory, Pasadena, California, pp. 1–12, February 15, 1990.
- [6] H. N. Royden, R. B. Miller, and I. A. Buennagel, "Comparison of NAVSTAR Satellite L-Band Ionospheric Calibrations with Faraday Rotation Measurements," *Radio Science*, vol. 19, no. 3, pp. 798–804, May–June 1984.
- [7] G. E. Lanyi and T. Roth, "A Comparison of Mapped and Measured Total Ionospheric Electron Content Using Global Positioning System and Beacon Satellite Observations," *Radio Science*, vol. 23, pp. 483–492, July–August 1988.
- [8] S. M. Lichten and W. I. Bertiger, "Demonstration of Sub-Meter GPS Orbit Determination and 1.5 Parts in  $10^8$  Three-Dimensional Baseline Accuracy," *Bulletin Geodesique*, vol. 63, no. 2, pp. 167–189, 1989.



- [9] A. P. Freedman, "Determination of Earth Orientation Using the Global Positioning System," *TDA Progress Report 42-99*, vol. July–September 1989, Jet Propulsion Laboratory, Pasadena, California, p. 1–11, November 15, 1989.
- [10] T. W. Hamilton and W. G. Melbourne, "Information Content of a Single Pass of Doppler Data from a Distant Spacecraft," *JPL Space Programs Summary 37-39*, vol. III, Jet Propulsion Laboratory, Pasadena, California, pp. 18–23, March–April 1966.

**Table 1. Assumed (one-sigma) Doppler random and systematic errors.**

| Parameter                       | Value |
|---------------------------------|-------|
| Data noise, mm/sec              | 0.1   |
| Wet zenith troposphere, cm      | 4     |
| Dry zenith troposphere, cm      | 1     |
| Daytime zenith ionosphere, cm   | 4     |
| Nighttime zenith ionosphere, cm | 2     |
| Station spin radius, cm         | 30    |
| Station longitude, cm           | 30    |
| Station z-height, m             | 5     |

**Table 2. Assumed tracking station coordinates.**

| Station/coordinate  | Value     |
|---------------------|-----------|
| <b>Goldstone</b>    |           |
| Spin radius, km     | 5203.997  |
| East longitude, deg | 243.1105  |
| z-height, km        | 3677.052  |
| <b>Australia</b>    |           |
| Spin radius, km     | 5205.251  |
| East longitude, deg | 148.9813  |
| z-height, km        | -3674.749 |

**Table 3. Initial state vector for near-zero-declination segment of Mars Observer trajectory.**

| Parameter                         | Value                    |
|-----------------------------------|--------------------------|
| Year                              | 1993                     |
| Day of year                       | 203 (22 July)            |
| Distance, km                      | $3.1573 \times 10^8$     |
| Right ascension ( $\alpha$ ), deg | 169.0252                 |
| Declination ( $\delta$ ), deg     | 5.1308                   |
| Radial velocity, km/sec           | 11.5770                  |
| $d\alpha/dt$ , deg/sec            | $6.2454 \times 10^{-6}$  |
| $d\delta/dt$ , deg/sec            | $-2.5866 \times 10^{-6}$ |

**Table 4. Line-of-sight position errors ( $1\sigma$ , km) for near-zero-declination trajectory.**

| $\sigma_D$ | $\sigma_e$   | $q$ | $\gamma_{min}$ , deg |       |       |       |       |       |       |       |
|------------|--------------|-----|----------------------|-------|-------|-------|-------|-------|-------|-------|
|            |              |     | 6                    | 10    | 15    | 20    | 25    | 30    | 35    | 40    |
| 0.1        | <b>NOISE</b> | ... | 31.8                 | 33.1  | 35.0  | 37.4  | 40.5  | 44.8  | 51.0  | 60.7  |
| 0.1        | 0            | ... | 184.8                | 119.3 | 90.7  | 79.3  | 73.9  | 71.1  | 70.8  | 74.9  |
| 0.2        | 0            | ... | 192.8                | 132.3 | 109.1 | 102.4 | 101.9 | 105.3 | 113.2 | 129.1 |
| 0.1        | 0.02         | 1   | 131.4                | 105.9 | 87.6  | 78.4  | 73.6  | 71.0  | 70.8  | 74.9  |
| 0.1        | 0.02         | 2   | 81.7                 | 80.7  | 78.3  | 75.2  | 72.6  | 70.8  | 70.8  | 75.0  |
| 0.1        | 0.02         | 3   | 72.7                 | 72.7  | 72.5  | 72.0  | 71.2  | 70.5  | 70.9  | 75.2  |
| 0.1        | 0.03         | 1   | 115.9                | 99.2  | 85.5  | 77.7  | 73.4  | 71.0  | 70.8  | 75.0  |
| 0.1        | 0.03         | 2   | 78.1                 | 77.5  | 76.1  | 74.0  | 72.1  | 70.7  | 70.9  | 75.1  |
| 0.1        | 0.03         | 3   | 72.2                 | 72.2  | 72.1  | 71.8  | 71.3  | 70.9  | 71.5  | 75.7  |
| 0.1        | 0.01         | 3   | 75.6                 | 75.5  | 75.0  | 73.8  | 72.1  | 70.6  | 70.7  | 74.9  |
| 0.1        | 0.05         | 3   | 72.7                 | 72.7  | 72.6  | 72.5  | 72.2  | 72.0  | 72.7  | 76.8  |

**Table 5. Initial state vector for high-declination segment of Mars Observer trajectory.**

| Parameter                         | Value                    |
|-----------------------------------|--------------------------|
| Year                              | 1993                     |
| Day of year                       | 113 (23 April)           |
| Distance, km                      | $1.9289 \times 10^8$     |
| Right ascension ( $\alpha$ ), deg | 120.1785                 |
| Declination ( $\delta$ ), deg     | 20.2819                  |
| Radial velocity, km/sec           | 18.4554                  |
| $d\alpha/dt$ , deg/sec            | $6.3462 \times 10^{-6}$  |
| $d\delta/dt$ , deg/sec            | $-1.0732 \times 10^{-6}$ |

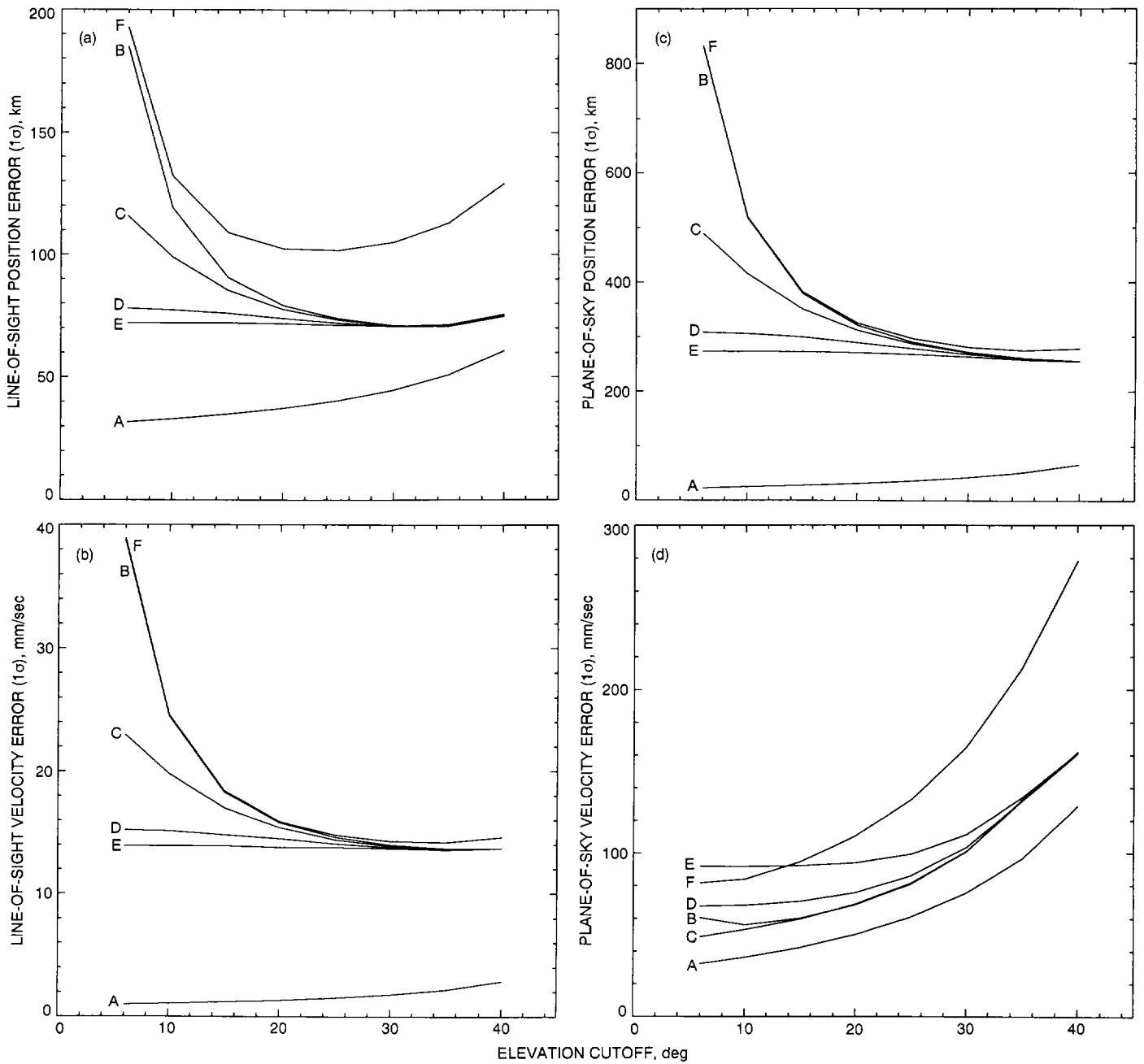


Fig. 1. Estimated errors as functions of elevation-angle cutoff for different weighting functions for the near-zero-declination segment of the Mars Observer trajectory, assuming two-way 8.4-GHz Doppler data acquired at Goldstone: (a) line-of-sight position error; (b) line-of-sight velocity error; (c) plane-of-sky position error; and (d) plane-of-sky velocity error.

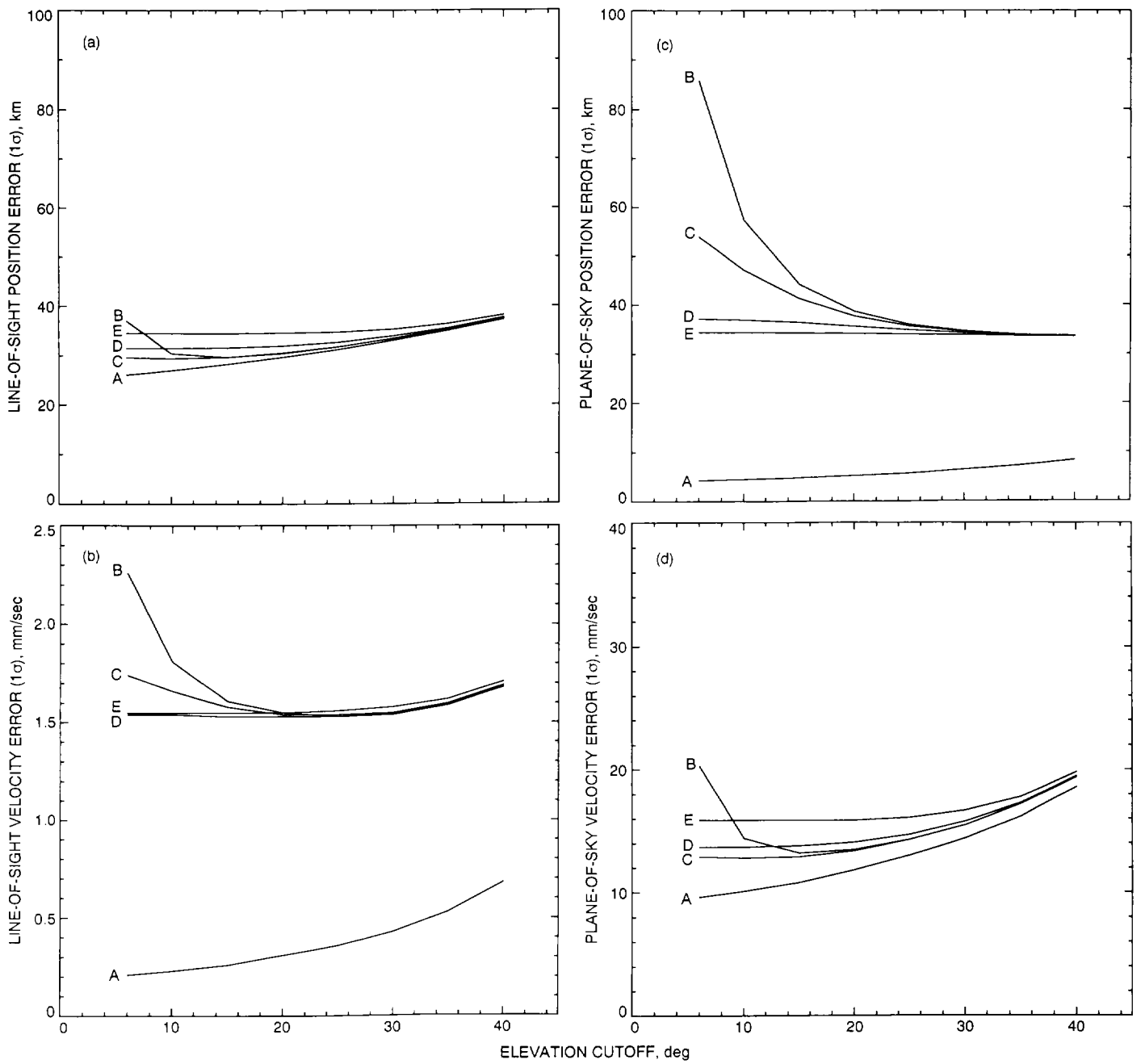
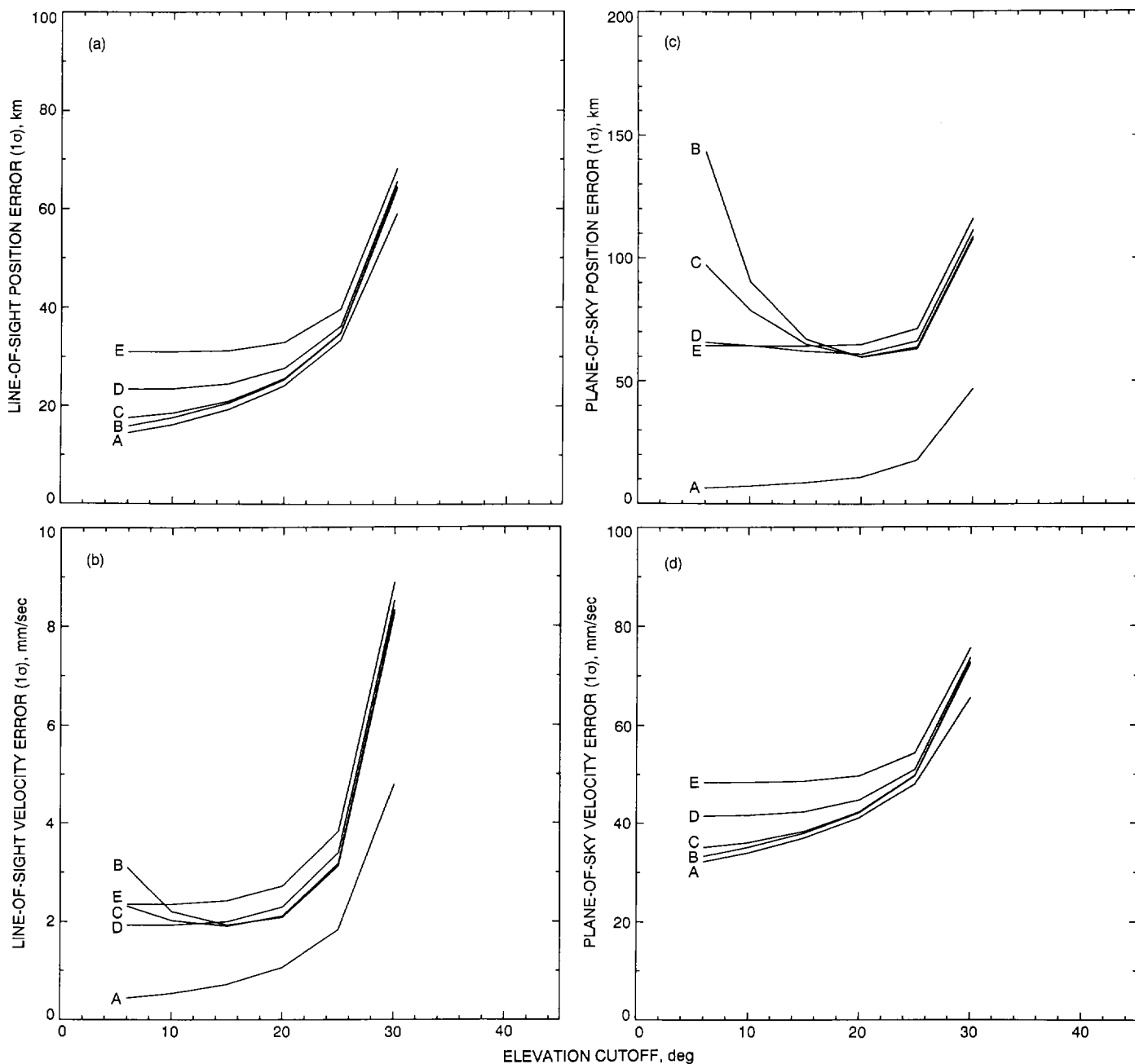
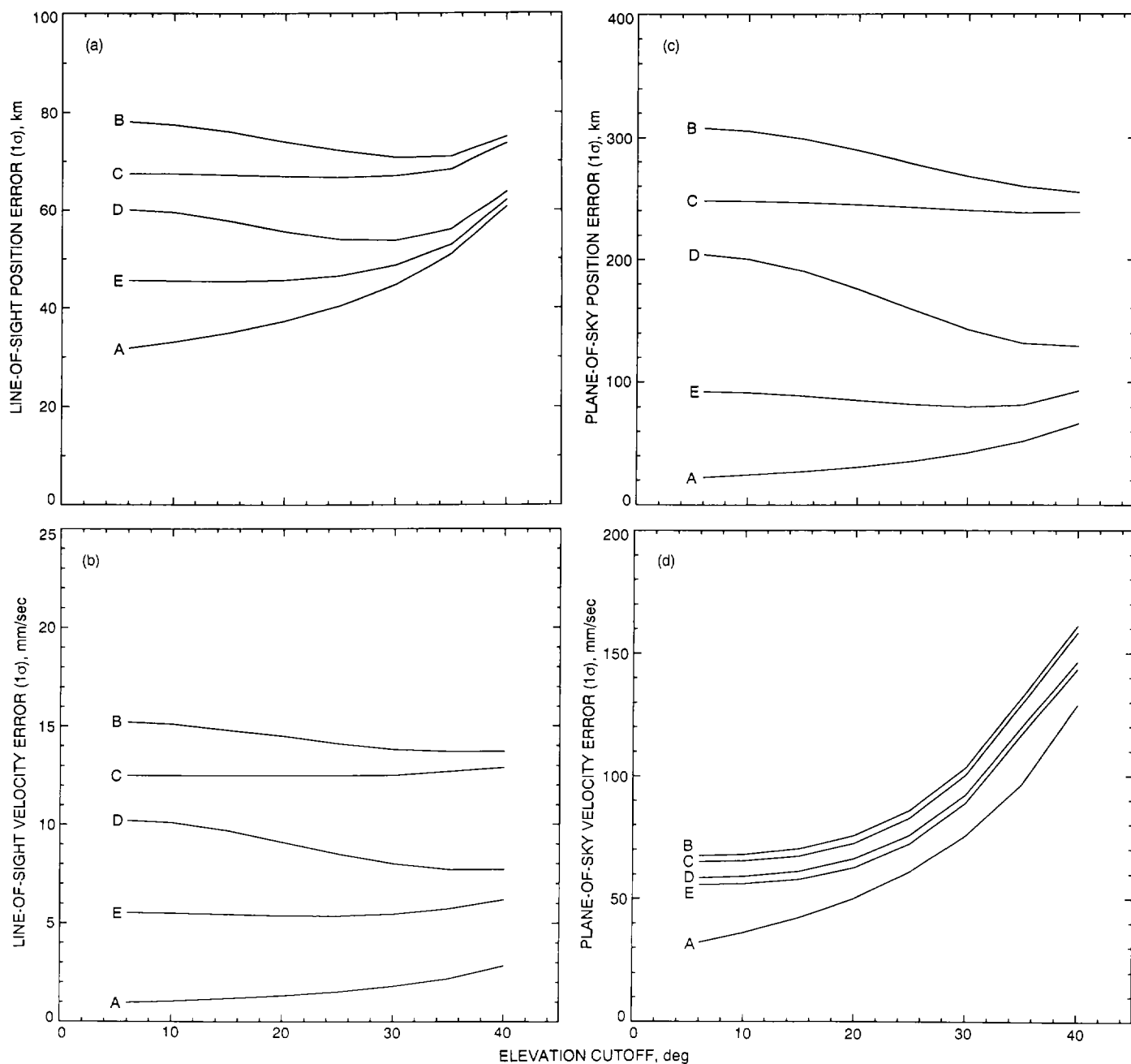


Fig. 2. Errors for the high-declination trajectory segment for Goldstone Deep Space Station. The weighting functions are the same as those used in Fig. 1, except the uniform deweighting to 0.2 mm/sec is not shown: (a) line-of-sight position error; (b) line-of-sight velocity error; (c) plane-of-sky position error; and (d) plane-of-sky velocity error.



**Fig. 3. Errors for the high-declination trajectory segment for Tidbinbilla Deep Space Station; weighting functions are the same as those used for Fig. 2: (a) line-of-sight position error; (b) line-of-sight velocity error; (c) plane-of-sky position error; and (d) plane-of-sky velocity error.**



**Fig. 4.** Errors for the near-zero-declination Mars Observer trajectory segment, tracked from Goldstone, for different improvements in the calibration: (a) line-of-sight position error; (b) line-of-sight velocity error; (c) plane-of-sky position error; and (d) plane-of-sky velocity error.

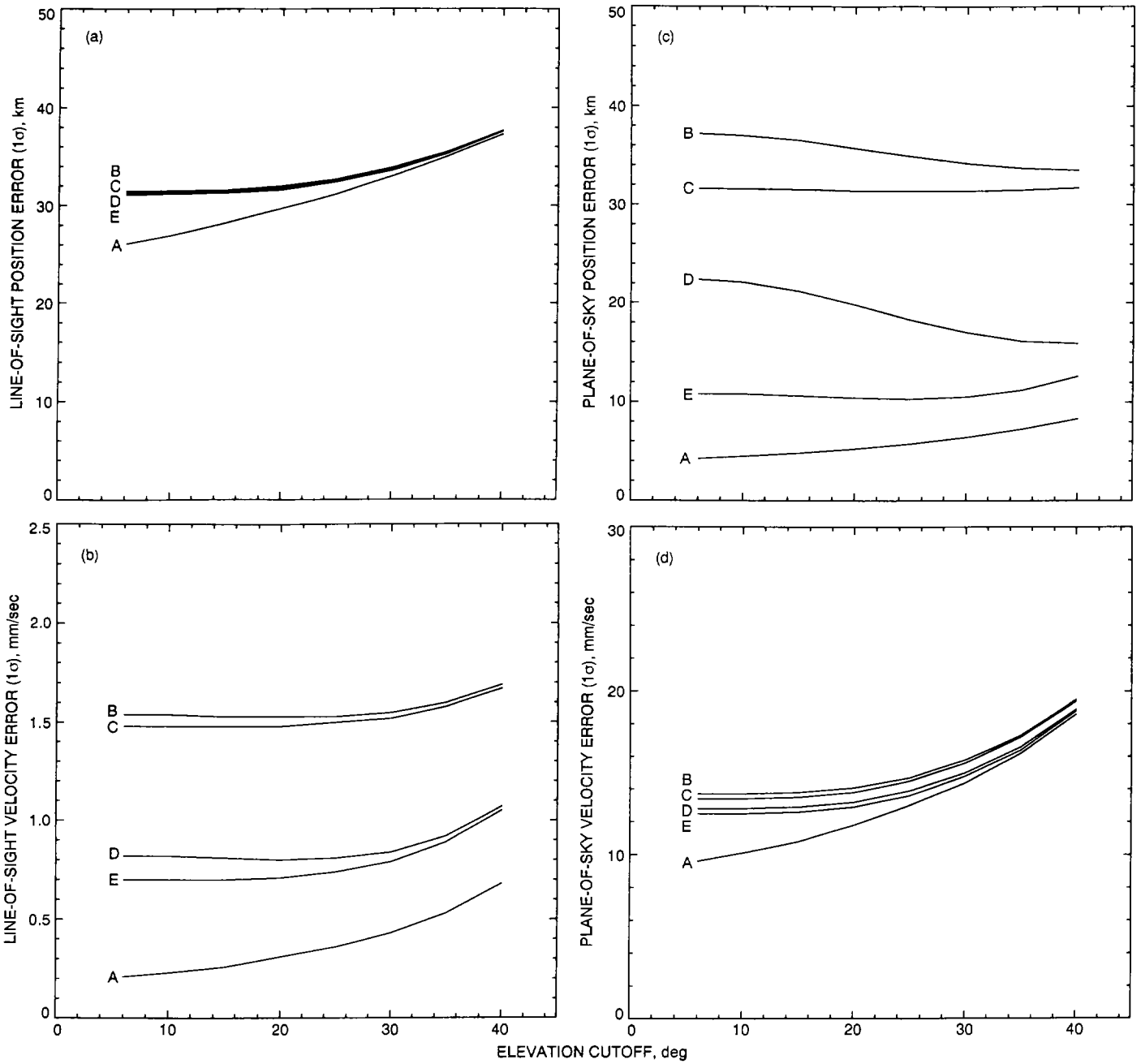
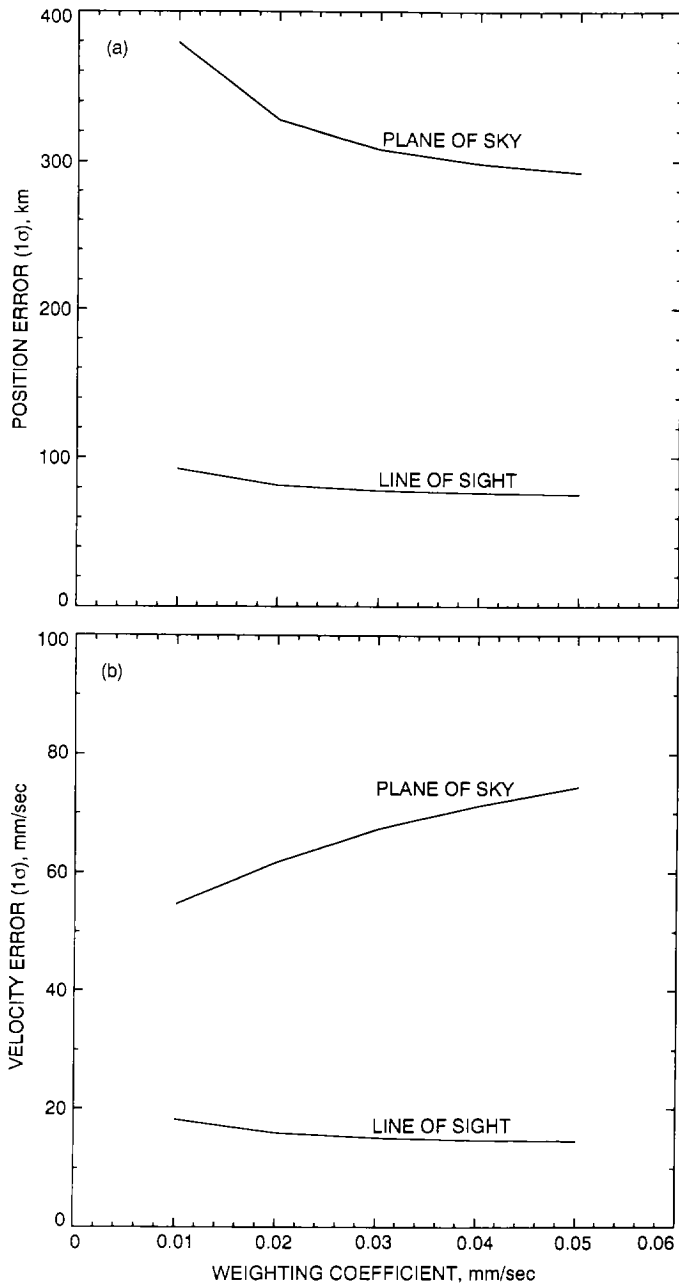


Fig. 5. Errors for the high-declination trajectory segment, tracked from Goldstone, for different improvements in the calibration: (a) line-of-sight position error; (b) line-of-sight velocity error; (c) plane-of-sky position error; and (d) plane-of-sky velocity error.





**Fig. 6. The dependence of predicted position and velocity accuracies on  $\sigma_\theta$ : (a) the dependence of the line-of-sight and plane-of-sky position errors versus  $\sigma_\theta$  and (b) dependence of line-of-sight and plane-of-sky velocity errors versus  $\sigma_\theta$ .**